SI Materials and Methods

Reagents and Antibodies

Primary antibodies used in this study include the following: rabbit monoclonal anti-Drp1, anti-phospho-Drp1 (S637), and anti-phospho-Drp1 (S616) (Cell Signaling); rabbit monoclonal anti-Mff (Sigma); rabbit polyclonal and mouse monoclonal anti-Parkin (Abcam); rabbit polyclonal anti-GAPDH (Santa Cruz); rabbit polyclonal anti-β-actin (Cell Signaling); mouse monoclonal anti-TOM20 (BD); rabbit polyclonal anti-TOM20 (Abcam); rabbit monoclonal anti-cleaved PARP and anti-cleaved caspase-3 (Cell Signaling); rabbit polyclonal anti-cytochrome c (Cell Signaling); HCV Core (Thermo Scientific); HCV NS5A (gift from Dr. Charles Rice, Rockefeller University, NY); HCV E2 (gift from Dr. Mansun Law, The Scripps Research Institute, CA). The secondary antibodies used for immunofluorescence were Alexa Fluor 405, 488, 594 or 647 donkey anti-mouse, rabbit, or goat IgG (Molecular Probe) and Alexa Fluor 555 goat anti-human IgG (Molecular Probe). The HRP-conjugated secondary antibodies used for Western blot analysis were from Cell Signaling Technologies and Jackson Laboratories.

siRNA Transfection

Small interfering RNA (siRNA) pools used in this study were siGENOME SMARTpool for Drp1, Parkin, CDK1, and non-targeting #1 control (Dharmacon). The cells were transfected with siRNA (30 nM) for the indicated times using DharmaFECT 4 transfection reagent according to the manufacturer's instructions (Dharmacon).

Real-time qRT-PCR

Quantitative real-time PCR analysis of HCV RNA levels was performed as described previously (1). The mRNA level of Drp1 was quantified by real-time qRT-PCR using DyNAmo HS SYBR Green qPCR kit (Finnzymes). The primers used were: Drp1 forward, 5'-TGGGCGCCGACATCA; Drp1 reverse, 5'-GCTCTGCGTTCCCACTACGA; GAPDH forward, 5'-GCCATCAATGACCCCTTCATT; and GAPDH reverse, 5'-TTGACGGTGCCATGGAATTT.

HCV RNA Replication and Foci-forming Unit (FFU) Assay

HCV RNA replication was determined by estimating the levels of HCV RNA in total cellular RNA by quantitative real-time PCR as described previously (2). Virus titer in the culture medium and cells was determined by FFU assay as described previously (2). Briefly, log-fold dilutions of the infectious cell culture medium were used to infect naïve Huh7.5.1 cells. 72 h post-infection the cells are fixed, immunostained for HCV NS5A and number of HCV positive foci counted. For intracellular infectivity, the cells were subjected to repeated freeze-thaw cycles and clarified cell lysate was used to perform FFU assay (2).

Glycolysis and ATP Estimation

Huh7 cells were transfected with non-targeting or gene-specific siRNAs against Drp1 or Mff. At 12 hours post-transfection, cells were infected with high titer (MOI ~5) of HCVcc. At 72 hours post-infection, cells and culture medium were collected. Glycolysis rate was estimated by determining the lactate levels in culture medium using the glycolysis cell-based assay kit according to the manufacturer's instructions (Cayman Chemicals). Total ATP levels were determined by luciferase-based ATP Enzylight kit according to manufacturer's instructions (BioAssay System).

Western Blot Analysis

For Western blot analysis, whole lysates were extracted from cells and homogenized liver biopsy tissues subjected to SDS-PAGE, transferred to nitrocellulose membrane (Thermo Scientific), and Western blot analyzed with antibodies against the indicated proteins as described previously (1).

Subcellular Fractionation

To isolate pure cytosolic and mitochondrial fraction, HCV-infected Huh7 cells were homogenized and isolated as described previously (1, 3).

Electron Microscopy

Huh7 cells infected with HCVcc at an MOI of 5 were prepared for electron microscopy. At 5 days post-infection, cells were fixed and embedded as described previously (1). Ultrathin sections were examined using a JEOL 1200 EX II transmission electron microscope at 80 kV.

ISRE-luciferase Reporter Assay

Briefly, Huh7 cells were cotransfected with a pISRE-Luc (a gift from Dr. Michael David, University of California, San Diego), expressing *firefly* luciferase under the transcriptional control of IFN-stimulated response element (ISRE), and pRL-CMV plasmids (Promega), expressing *Renilla* luciferase. Subsequently, these cells were transfected with non-targeting (NT) or gene specific siRNA pools targeting Drp1 and infected with HCVcc (MOI of 5) 12 h later. At 2 days post-infection, the relative ISRE-luciferase activity was determined by using the dual-luciferase reporter assay system according to the manufacturer's instructions (Promega). Firefly luciferase activity was normalized against *Renilla* luciferase activity to normalize the transfection efficiency.

Caspase-3/7 and TUNEL assay

The activity of caspase-3/7 in HCV-infected cells transfected with siRNA pools specific to Drp1 and Parkin, respectively, was measured by using Caspase-Glo 3/7 assay kit according to the manufacturer's instructions (Promega). Apoptotic cell death in these cells *was* measured by using Click-iT TUNEL Alexa Fluor 488 imaging assay kit according to the manufacturer's instructions (Invitrogen). For quantitative analysis, at least 1,000 cells on immunofluorescence image were counted.

Human liver biopsy specimens

The frozen human liver biopsy specimens (n = 3) were obtained from UCSD medical center. The liver biopsy specimens used in this study include the following: anti-HCV negative normal patient, n = 1; anti-HCV positive patients with chronic HCV, n = 2. The biopsy material was collected on

consent of the patients following the institution ethical guidelines.

Statistical Analysis

Statistical analysis using the unpaired Student *t* test was performed by using Sigma Plot software (Systat Software Inc., San Jose, CA).

References

1. Kim SJ, Syed GH, & Siddiqui A (2013) Hepatitis C virus induces the mitochondrial translocation of Parkin and subsequent mitophagy. *PLoS Pathog* 9(3):e1003285.
2. Syed GH & Siddiqui A (2011) Effects of hypolipidemic agent nordihydroguaiaretic acid on lipid droplets and hepatitis C virus. *Hepatology* 54(6):1936-1946.
3. Wieckowski MR, Giorgi C, Lebiedzinska M, Duszynski J, & Pinton P (2009) Isolation of mitochondria-associated membranes and mitochondria from animal tissues and cells. *Nat Protoc* 4(11):1582-1590.

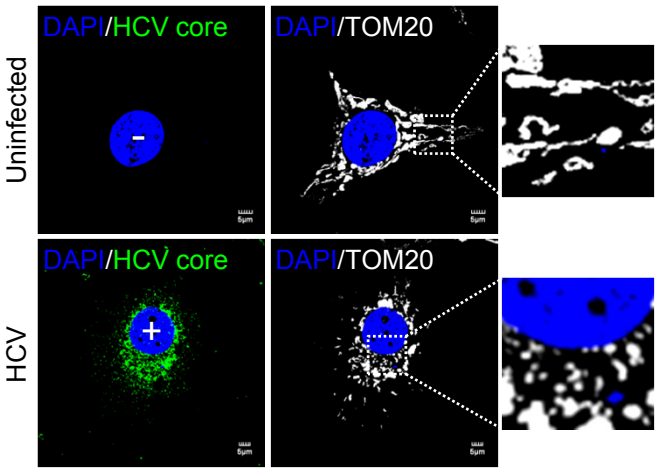

Fig. S1. HCV infection promotes mitochondrial fission. Confocal image of HCV-infected cells showing mitochondrial fission. Huh7 cells infected with JFH1 HCVcc were immunostained with antibodies specific to TOM20 (white) and HCV core protein (green). Nuclei were stained with DAPI (blue). Infected (+) and uninfected (-) cells are marked. In the zoomed images, fragmented mitochondria in HCV-infected cells and typical tubular mitochondria in uninfected cells are shown.

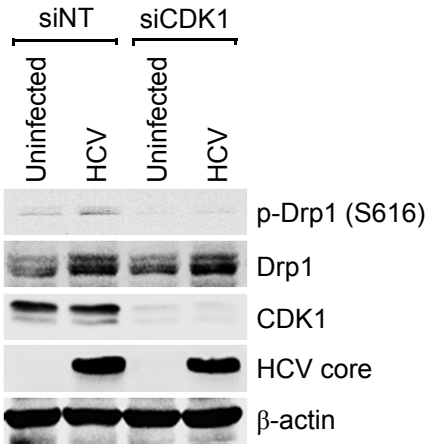

Fig. S2. Silencing CDK1 suppresses HCV-induced Drp1 Ser616 phosphorylation. Huh7 cells infected with HCVcc were transfected with non-targeting (NT) or CDK1-specific siRNA pools. At 3 days post-transfection, whole cell lysates were analyzed by immunoblotting with antibodies specific to the indicated proteins. β-actin, internal loading control.

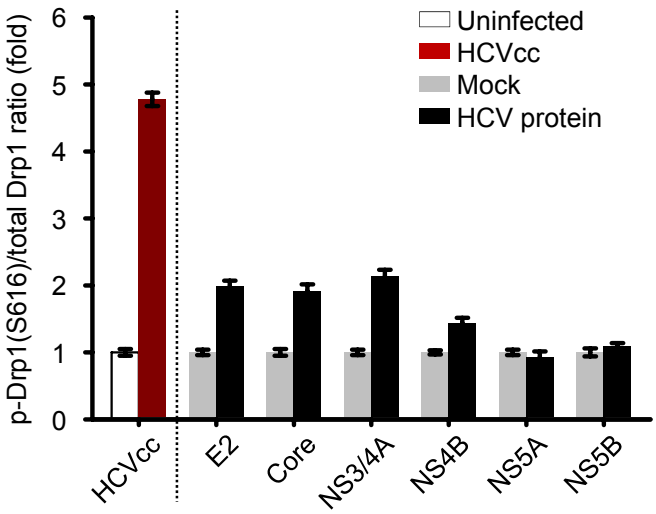

Fig. S3. HCV proteins-mediated Drp1 Ser616 phosphorylation. The intensity ratio of p-Drp1(S616)/total Drp1 analyzed by ImageJ software. The expression levels of p-Drp1 (S616) and total Drp1 were analyzed by immunoblotting of whole cell lysates extracted from Huh7 cells transiently expressing HCV E2, core, NS3/4A, NS4B, NS5A, and NS5B, respectively. Mock, empty vector.

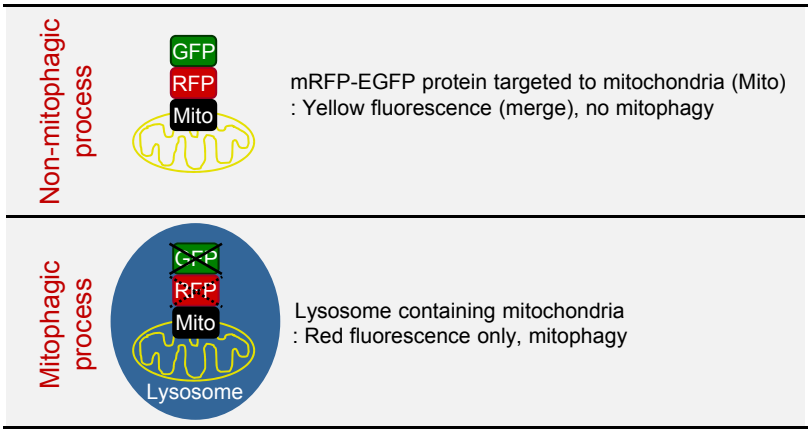

Fig. S4. A novel system for monitoring mitophagy. A Novel system for monitoring the maturation process by which mitophagosomes are converted into mitophagolysosome (mitophagy) using a dual fluorescence p-mito-mRFP-EGFP reporter. Lysosomal delivery of the tandem fusion protein mito-mRFP-EGFP along with entire mitochondria results in differential quenching and degradation of the two individual fluorochromes, thereby allowing for visual analysis of mitophagic flux.

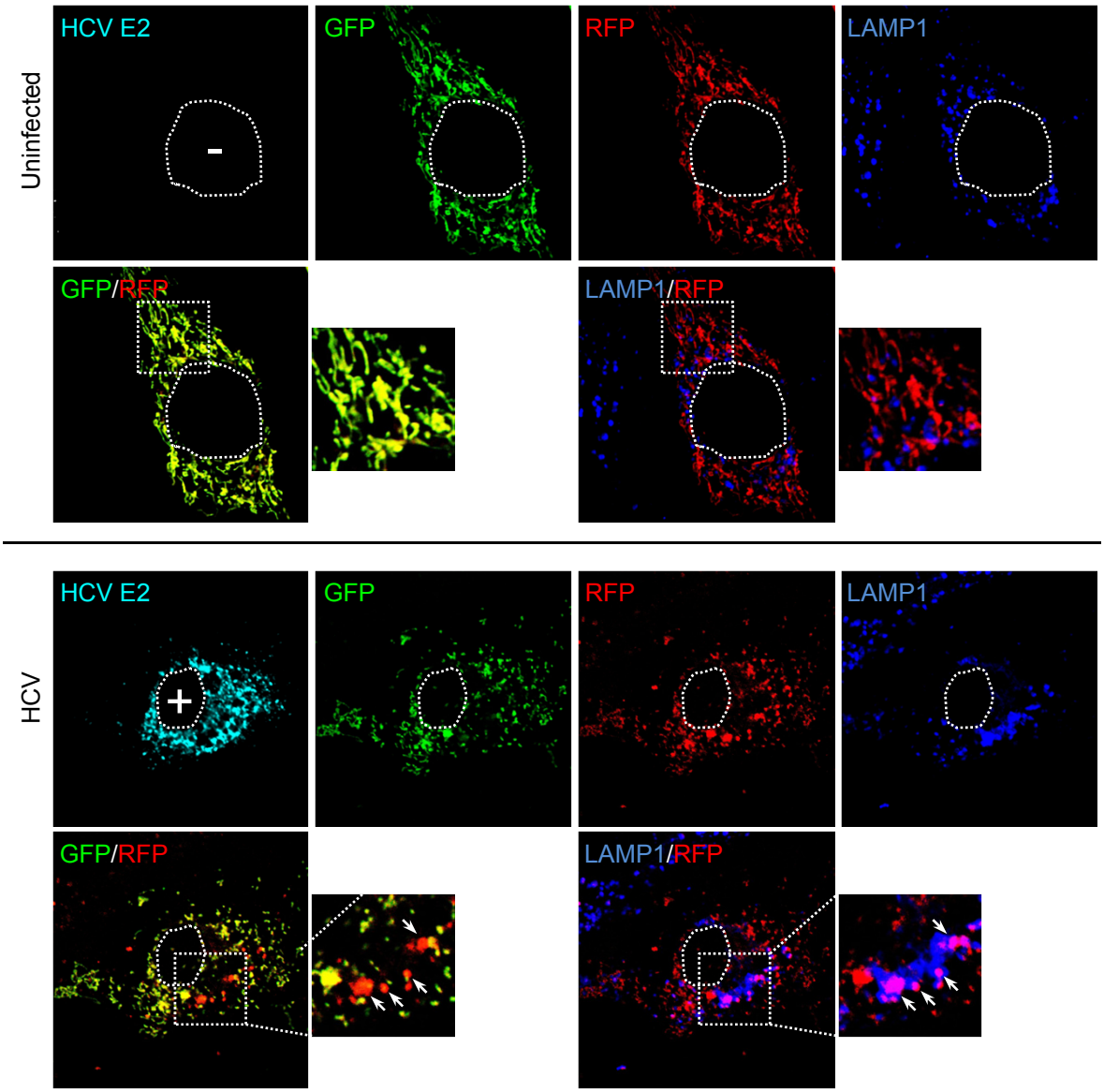

Fig. S5. HCV induces complete mitophagy. Confocal images showing the fusion between mito-mRFP-EGFP and lysosome (mitophagolysosome formation) in HCV-infected cells. Uninfected and infected cells transiently expressing mito-mRFP-EGFP were immunostained with antibodies specific to LAMP1 (blue) and HCV E2 protein (cyan). Nuclei, white dot circles. Uninfected cells, (-); infected cells (+). In the zoomed images, the arrows indicate merged of red fluorescence of mito-mRFP-EGFP targeted to mitochondria with lysosome (pink puncta).

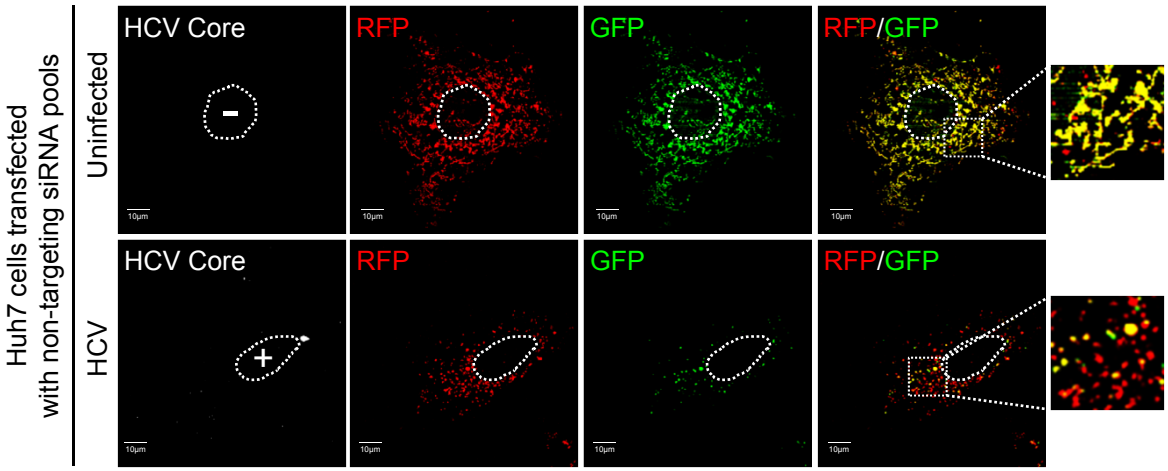

Fig. S6. Confocal images showing mitophagy in HCV-infected cells in the presence of non-targeting siRNA. At 2 days post-infection, HCV-infected cells transiently expressing mito-mRFP-EGFP were immunostained with anti-HCV core antibody (white). Nuclei, white dot circles. Infected cells, (+); uninfected cells, (-). The zoomed images display tubular mitochondrial network in uninfected cells and fragmented mitochondria in infected cells.

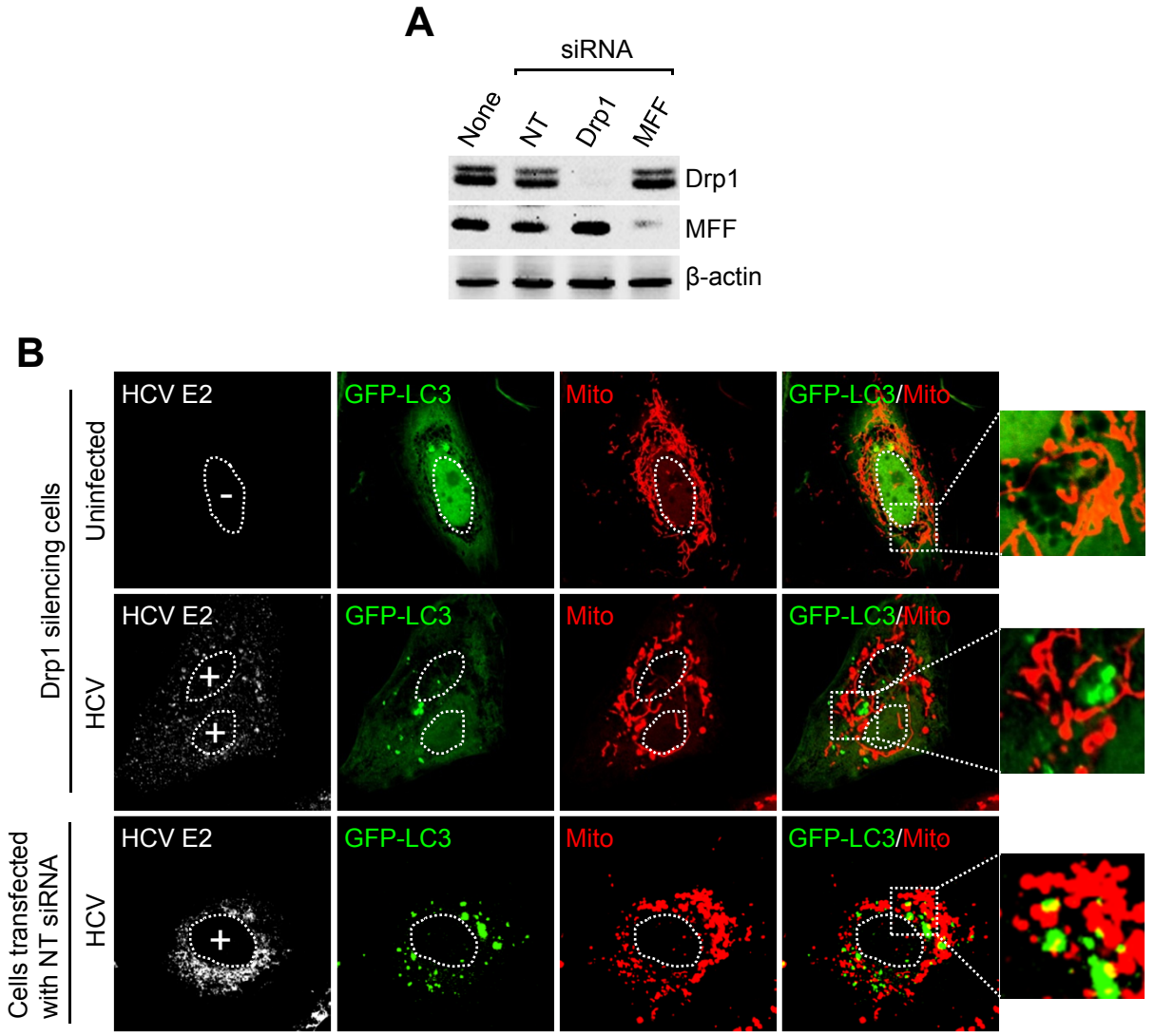

Fig. S7. Drp1 silencing interferes with mitophagosome formation in HCV-infected cells. (*A*) Western blot analysis of whole cell lysates extracted from Huh7 cells transfected with siRNA pools specific to Drp1 and Mff, respectively. Non-targeting (NT) siRNA pools, a negative control. (*B*) Confocal microscopy showing inhibition of mitophagosome formation by silencing Drp1 in HCV-infected cells. Drp1-silencing Huh7 cells transfected with GFP-LC3 construct were infected with HCVcc. At 2 days post-infection, cells prestained with MitoTracker (Mito, red) were immunostained with anti-HCV E2 antibody (white). Infected cells, (+); uninfected cells, (-). Nuclei, white dot circles. The zoomed image indicates that GFP-LC3 puncta (green) does not colocalize with mitochondria in HCV-infected cells.

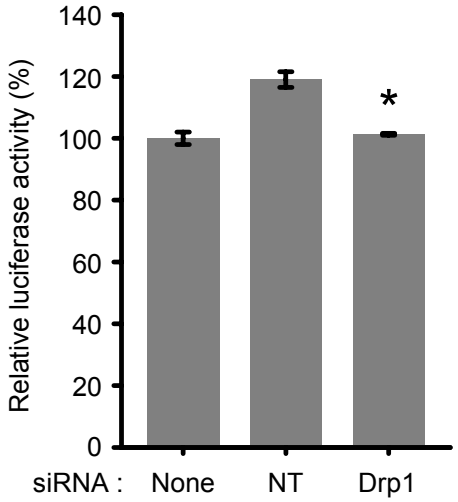

Fig. S8. Drp1 silencing does not affect HCV replication. SGR-Feo subgenomic replicon cells were transfected with non-targeting (NT) or Drp1-specific siRNA pools (30 nM) and assayed at 2 days post-transfection. Values are mean ± SD (n = 3). *$P \leq$ 0.05, by unpaired Student t test.

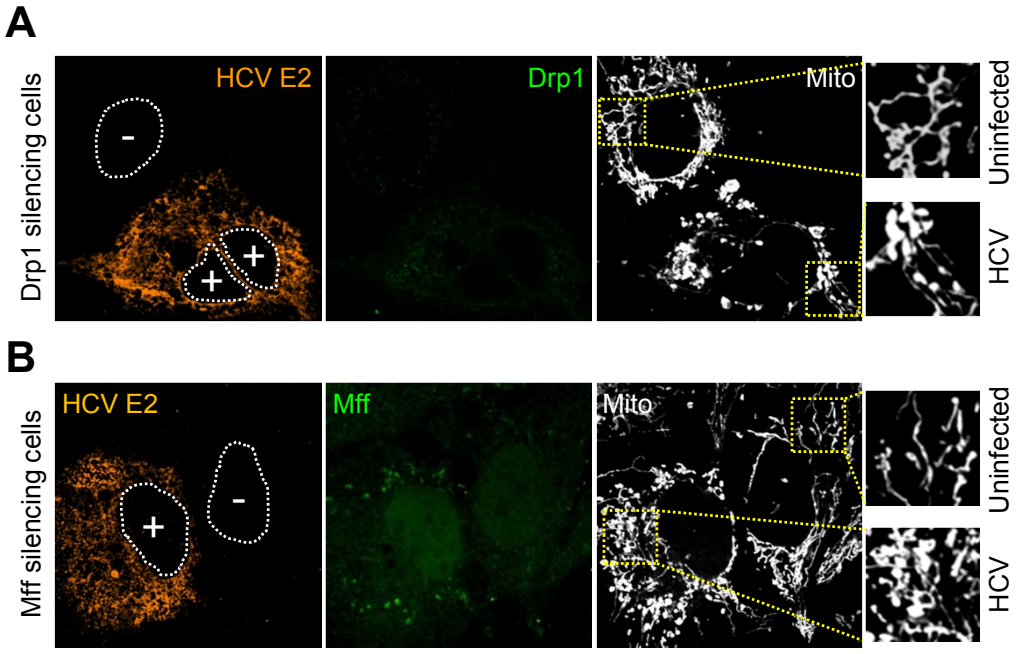

Fig. S9. Drp1 and Mff silencing enhances HCV-induced mitochondrial swelling. (*A* and *B*) Confocal microscopy showing mitochondria shape with enhanced swelling morphology in Drp1 (*A*) or Mff (*B*) silencing HCV-infected cells. Huh7 cells transfected with Drp1 and Mff siRNA, respectively were infected with HCVcc (MOI of 1). At 2 days post-infection, cells prestained with MitoTracker (Mito, white) were immunostained with antibodies specific to Drp1 (green, panel *A*), Mff (green, panel *B*), and HCV E2 protein (orange). In the zoomed images, uninfected cells display tubular mitochondria, whereas infected cells show tubular and enhanced mitochondrial swelling. Infected cells, (+); uninfected cells, (-). Nuclei, white dot circles.

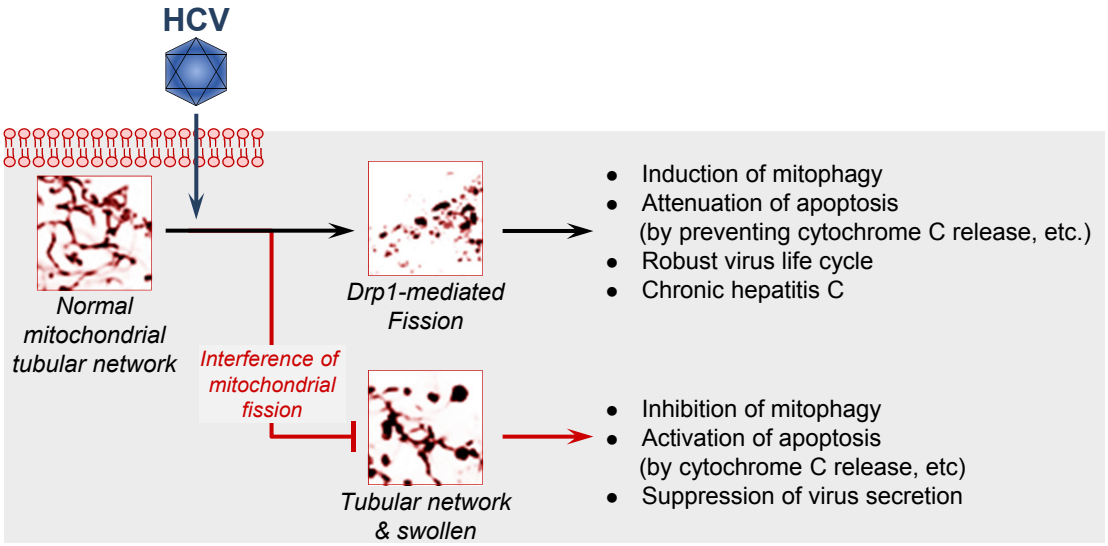

Fig. S10. A model elucidating the role of HCV-induced mitochondrial fission in mitochondrial apoptosis and viral life cycle. HCV infection disrupts mitochondrial dynamics: Induces mitochondrial fission via Drp1 translocation to mitochondria subsequent mitophagy. Interference of mitochondrial fission can lead to apoptotic cell death in infected cells via upregulation of apoptotic signaling as shown in Fig. 5.

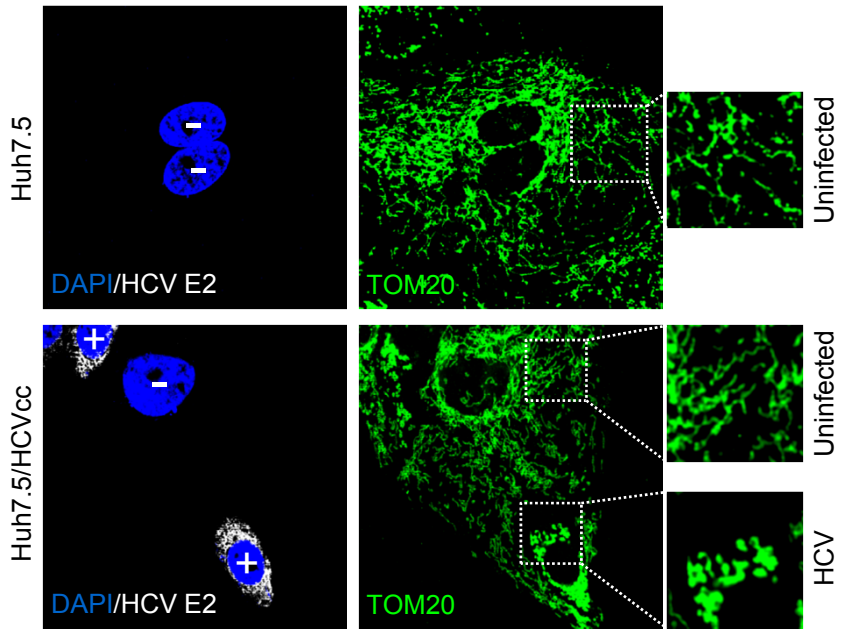

Fig. S11. HCV induces mitochondrial fission in Huh7.5 cells. Confocal microscopy showing mitochondrial fission in HCV-infected Huh7.5 cells. At 2 days post-infection, Huh7.5 cells infected with HCVcc (MOI of 1) were immunostained with antibodies specific to TOM20 (green) and HCV E2 protein (white). Nuclei, DAPI (blue). Infected cells, (+); uninfected cells, (-). The zoomed images display tubular mitochondrial network in uninfected cells and fragmented mitochondria in infected cells.